Solid State Phenomena
ISSN: 1662-9779, Vol. 389, pp 65-74
doi:10.4028/p-P58jF8

Submitted: 2025-12-04
Revised: 2026-02-20
Accepted: 2026-02-24
Online: 2026-04-16

Numerical Study of Process-Specific Disturbances in Hollow Embossing Rolling

Franz Reuther[1,a*], Verena Psyk[1,b] and Verena Kräusel[1,c]

[1]Fraunhofer Institute for Machine Tools and Forming Technology, Reichenhainer Strasse 88, 09126 Chemnitz, Germany

[a*]franz.reuther@iwu.fraunhofer.de, [b]verena.psyk@iwu.fraunhofer.de, [c]verena.kraeusel@iwu.fraunhofer.de

*corresponding author

Keywords: simulation, bipolar plates, hollow embossing rolling, disturbances.

Abstract. Hollow embossing rolling (HER) is a promising continuous forming technology for producing thin metallic bipolar half plates (BPHP) with micro-channel structures used in fuel cells and electrolyzers. This study presents a simulation-based analysis of process-specific disturbances influencing the forming accuracy and quality of HER-formed BPHP. Using a validated LS-DYNA shell-based model, the effects of six disturbance variables, roller misalignments (axial, tangential, angular), roller gap variation, initial sheet thickness deviation, and changes in friction coefficient, were systematically investigated. Results show that even small roller misalignments of ±10 µm or manufacturing related roller gap deviations of +5 µm lead to significant changes in rolling force, strip draw-in, and sheet thinning behavior. Variations in friction coefficient notably affect draw-in and wrinkling tendencies. Overall, the study highlights the high sensitivity of the HER process to geometric and frictional disturbances and provides quantitative tolerance limits crucial for precision manufacturing and robust continuous BPHP forming.

Introduction

Hollow embossing rolling (HER) is a promising technology for continuous high rate forming of bipolar half plates – BPHP, i. e. thin metallic plates used as media distributors in fuel cell stacks [1] or electrolyzers [2]. Based on several preliminary studies with different approaches to the continuous rolling of complex channel geometries [3,4], this process approach has been significantly enhanced over the past five years. The starting point for this development was a series of numerical studies for designing, validating, and optimizing a basic virtual model approach [5]. This enabled not only the transfer of the validated models to full-scale plates [6], but also the experimental verification of the process [7] on specially developed rolling machines at the Fraunhofer Institute for Machine Tools and Forming Technology IWU [8]. The advantages of the HER process over conventional technologies such as hydroforming or stamping include significantly higher production rates due to continuous strip movement and in general lower forming forces, which enable a much more compact and cost-effective machine design [9]. However, forming ultra-thin metallic strips with thicknesses of 0.05–0.10 mm and micro-channel structures in the sub-millimeter range is still highly challenging. These boundary conditions require exceptionally high precision in the manufacturing of the embossing rollers, their alignment and their synchronous rotation. The aim of this study is the simulation-based evaluation of process-specific disturbances related to these process conditions in order to analyze their influence on the resulting quality of BPHP formed by HER and the derivation of tolerance requirements.

Simulation Set Up for Investigation of Disturbance Variables

A miniaturized BPHP geometry measuring 45 x 30 mm is used for the following investigations for which experimental and numerical investigations have already been published in Reuther et al. [5].

The testing geometry combines different flow field zones with trapezoidal channel cross-sections and geometric elements representing typical BPHP for PEM fuel cells (Fig. 1 a). The initial sheet thickness is t_0 = 0.1 mm.

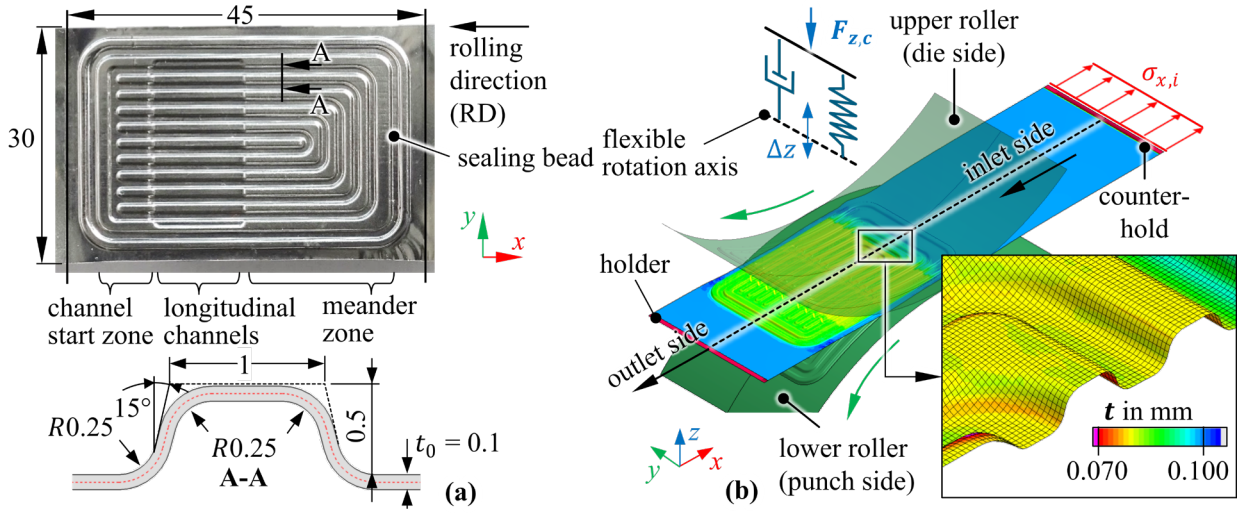

Fig. 1. Forming demonstrator BPHP: (a) experimental results of HER and geometry, (b) validated and optimized simulation model of hollow embossing rolling [5].

With the aim of a simulation-based investigation of disturbances in hollow embossing rolling on this BPHP geometry, a corresponding shell-based model was set up in LS-DYNA R12.1 (Fig. 1 b) using the already validated modelling approach presented in [5]. The rigid surface meshes of the forming rollers rotate synchronously with each other and gradually form the channel geometry into the sheet metal strip. This is fed under strip tension on the inlet side $\sigma_{x,i}$ = 100 N/mm² in order to prevent uncontrolled strip draw-in and therefore excessive wrinkling. Another key feature is the flexible definition of the rotation axes, which is implemented for each roller mesh using spring-damper elements. By defining a sufficiently large constant clamping force $F_{z,c}$ at the axis suspension of the upper roll, the strip can be carried along by the contacts in accordance with the experimental boundary conditions. Due to this flexible axis modelling, the effective rolling gap s_w does not remain constant at the initially specified value of $s_w = t_0$, but can change as a result of the current rolling force F_z caused by different local BPHP cross-sections (load-dependent rolling gap change Δs_w). Both aspects have been identified as important features for accuracy during model validation and are therefore also taken into account in this study. Based on the previous investigations [5], a static friction coefficient of μ_s = 0.25 is defined as first assumption. Further boundary conditions for modeling with regard to strip and roller meshing, as well as other setting parameters for explicit computation, are based on previously developed standards for shell-based simulation of HER with LS-DYNA [10]. Elastic-plastic material modelling of the strip material (austenitic stainless steel 1.4404) was implemented using an anisotropic material law with strain rate dependency based on uniaxial tensile tests at different strain rates and rolling direction orientations as well as bulge tests according to [5].

Definition of Disturbances and Evaluation Criteria

Based on this reference simulation setup, different disturbance variables are implemented separately in the reference model and the changes in the result variables are analyzed in order to systematically identify correlations. As shown in Fig. 2, a selection of six different disturbance variables is investigated: Misalignments of the upper roller mesh relative to the lower roller leading to changes in the rolling gaps between the rollers especially at the trapezoidal oriented channel flanks. A distinction is made here between **axial δ_y**, **tangential δ_x**, and **angular misalignment δ_α**. While axial misalignment primarily affects the existing rolling gap of channels oriented longitudinally to the rolling direction (RD), tangential and angular misalignment affects the rolling gap in channels

oriented transversely to the RD. Generally, no change is visible in the case of horizontally oriented cross-section areas (channel head and foot areas) as the roller meshes are only shifted horizontally to each other. In contrast, the **roller gap variation δs_w** symbolizes a geometrical change in the die roller due to assumed manufacturing inaccuracies. This change is defined in simple terms as homogeneous oversize, which is represented equally in the flat areas of the channel cross-sections and in the channel flanks. Positive values lead to a smaller effective rolling gap and vice versa. A similar effect is caused by a **variation in the initial sheet thickness δt_0**. With $t = t_0 + \delta t_0$ clamping effects in the rolling gap increase for $\delta t_0 > 0$, because the thicker strip is formed into the initial roller meshes of the reference simulation. Variations in the **static friction coefficient $\delta \mu_s$** are also investigated as a final disturbance variable. Since the contact and friction situation generally has major influence on the forming result in the microforming of BPHP-typical channel structures, it can be assumed that corresponding variations also significantly affect the results. Varying friction coefficients can be caused, for example, by different surface roughnesses of the rollers or strip materials or by an inhomogeneous lubricant supply, whereby these fluctuations cannot be sufficiently limited due to manufacturing or process-related factors.

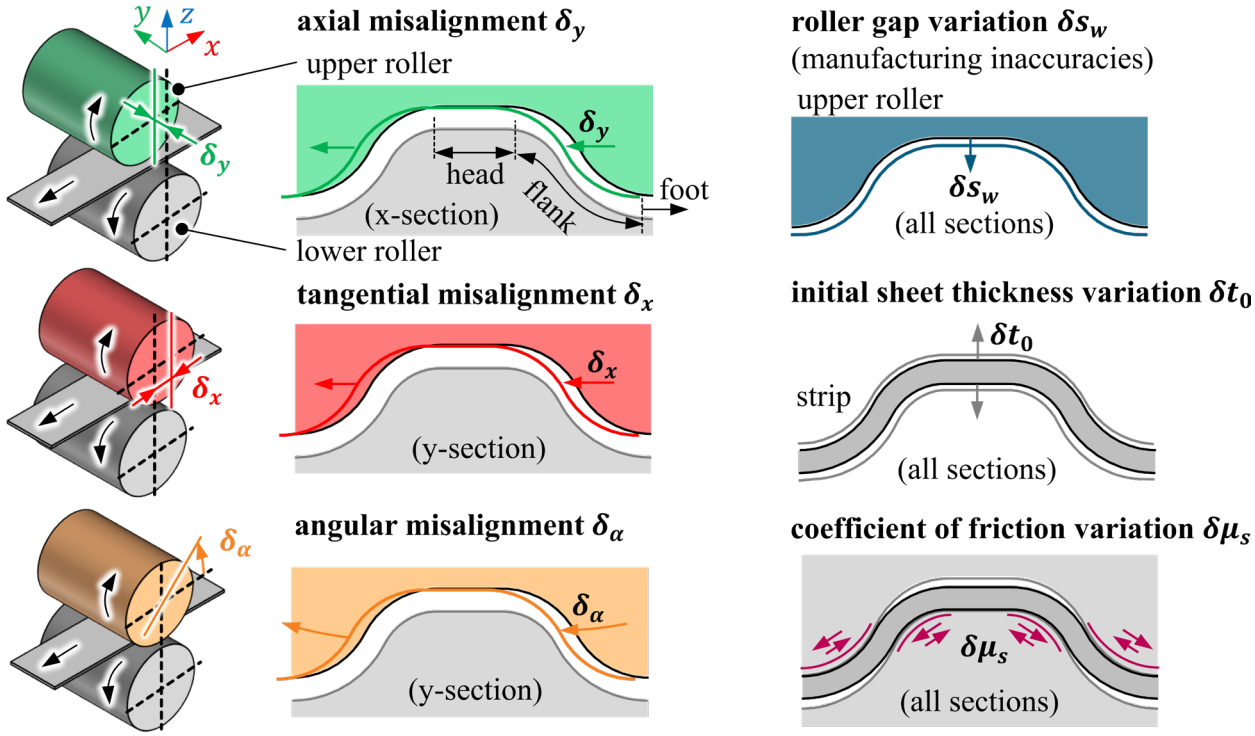

Fig. 2. Investigated disturbance variables: misalignments, variation of roller gap and initial thickness as well as coefficient of friction variation.

For the systematic analysis of the result changes, a range of process-specific evaluation variables are used, which are summarized in Table **1**. A change in the stretching behavior during channel forming is represented by the resulting sheet thickness variation Δt. Effects on strip draw-in and the associated wrinkling tendency are analyzed by transversal and longitudinal strip draw-in changes ($\Delta y_e, \Delta x_e$) as well as a wrinkle criterion $\Delta \varepsilon_{WT}$ according to [6]. In addition, there are possible changes in the rolling force ΔF_z during continuous channel forming. Geometric changes of the forming demonstrator are considered here as changes of the channel height Δh and the resulting flatness deviation $\Delta \delta_E$. The evaluation is carried out in accordance with the specifications in Table **1** and the listed threshold levels each defining the transition from a minor to a significant change in results. Usually, the results are analyzed by average values (e.g., $\overline{\Delta F_z}$) and the corresponding standard deviations. In order to highlight individual effects, some results are summarized by calculating the mean value only for individual sections (A, B, C, D), specific areas (x_1, x_2, x_3, x_4), or time periods (t_1, t_2, t_3, t_4), at which certain areas are to be formed (Fig. 3).

Table 1. Evaluation criteria with corresponding methods, reference and thresholds values.

result variable change	evaluation method	reference value	threshold level
strip thickness Δt in µm	section-based (A-D), separate evaluation of channel flanks, heads and foots [6]	25 µm (t_0 - t_{min})	±1µm (~5 %)
draw-in (transversal) Δy_e in mm	transversal draw-in of the strip edge (y-dir.), zone-based evaluation (x_{1-3})	0.4 mm ($y_{e,max}$)	±0.02 mm (~5 %)
draw-in (longitudinal) Δx_e in mm	longitudinal draw-in of the strip end (x-dir.), evaluation at different time periods (t_{1-3})	2.0 mm ($x_{e,max}$)	±0.10 mm (~5 %)
rolling force ΔF_z in kN	evaluation at different time periods (t_{1-3})	5 kN ($F_{z,max}$)	±0.25 kN (~5 %)
channel height Δh in µm	section-based (A-D)	0.5 mm (h_{max})	±5 µm (~ 1 %)
flatness deviation $\Delta\delta_E$ in mm according to [6]	deviation to target-geometry, separate evaluation for clamped an unclamped state	-	0.1 mm

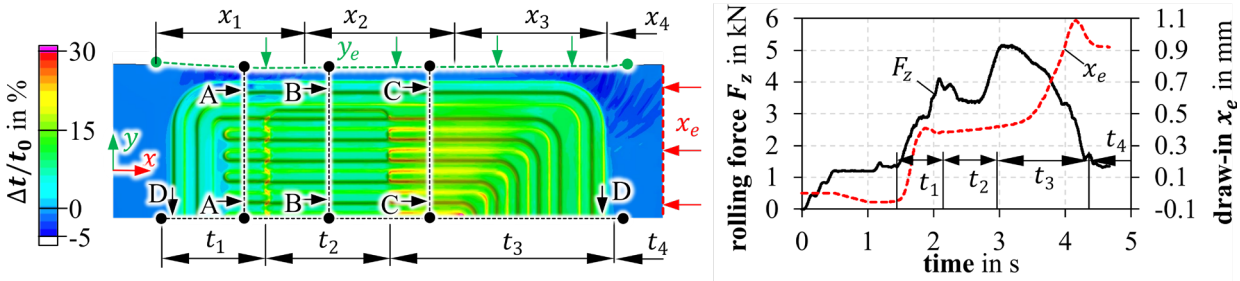

Fig. 3. Evaluation for BPHP testing geometry: section definition, zones and time periods.

Effects of Disturbance Variables on Evaluation Criteria and Discussion

Axial misalignment.

Assuming an axial misalignment δ_y of the upper roller of max. ±30 µm, several significant result changes can be observed compared to the reference simulation, which exceed the defined threshold level. The axial misalignment is first evident in the form of increasing rolling forces (Fig. 4 a). For δ_y > +20 µm and < -10 µm, significant rolling force changes occur throughout the entire channel forming period compared to the reference due to the locally reduced rolling gap in all areas with longitudinal channels (Fig. 4 b, time period t_2). The average transversal edge draw-in Δy_e is even more sensitive, being significantly lower for the middle part section x_2 even at an axial misalignment of δ_y ~ -5 µm. Changes in the edge draw-in are therefore a suitable evaluation criterion for identifying axial misalignment of the forming rollers experimentally. Due to the increased rolling forces (Fig. 4 c), axial misalignment is also accompanied by increasing rolling gap changes (on average +0.7 µm at δ_y = -20 µm). The average sheet thickness change in the channel flanks is small according to Fig. 4 a, but the large standard deviations also indirectly indicate a significant influence here. The alternating decrease and increase in the rolling gap in the successive channel flanks of longitudinal channels results in alternating larger and smaller thinning effects. Even at δ_y = -5 µm, changes in the maximum thinning in the channel flanks of ±5 µm (~ ±5 %) can be detected on average, which is a relevant order of magnitude, particularly regarding forming limits and crack formation in the channel flanks. The thinning of adjacent flanks of longitudinal channel structures with identical cross-sections can therefore also be used as an evaluation criterion to quantify axial misalignments of the forming rollers experimentally.

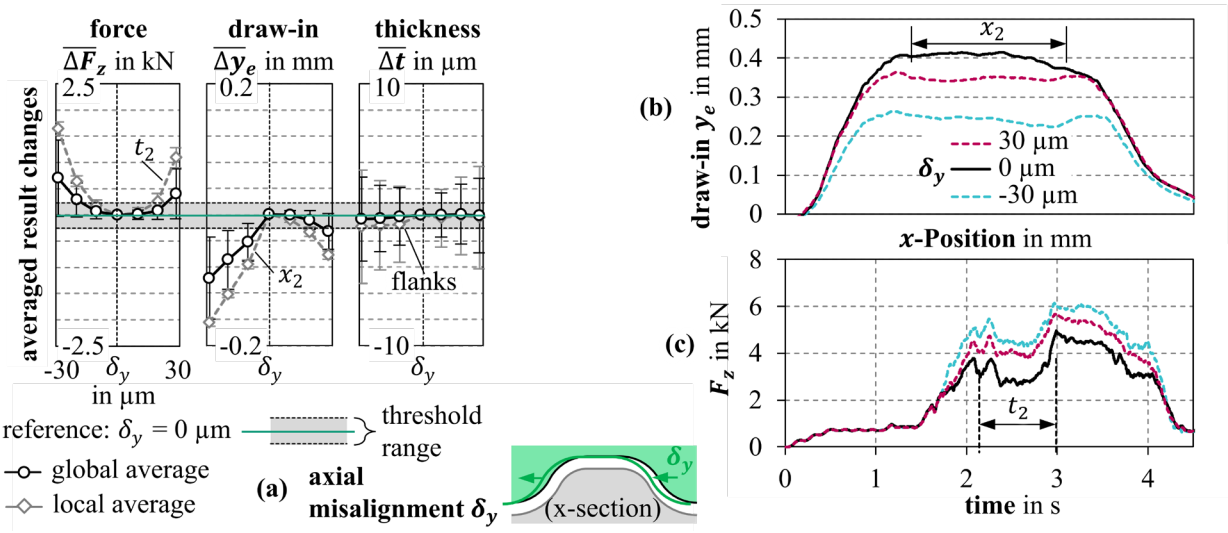

Fig. 4. Effects of axial misalignment: (a) significant changes of evaluation criteria, (b) exemplary change of transversal draw-in, (c) exemplary change of rolling force.

Tangential misalignment.

With a tangential misalignment δ_x of the forming rollers the locally smaller rolling gaps at transversal channels lead to increased rolling forces, which can be seen, for example, for δ_x = ±30 µm, for time periods t_1 and t_3 (Fig. 5 b).

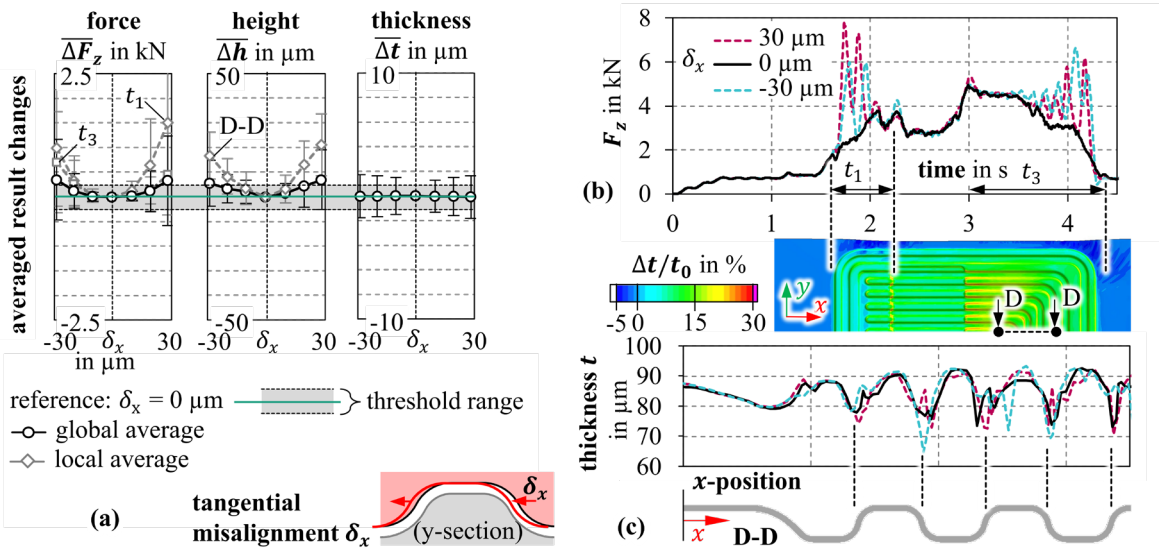

Fig. 5. Effects of tangential misalignment: (a) significant changes of evaluation criteria, (b) exemplary change of rolling force, (c) exemplary change of thickness in longitudinal section D.

For these evaluation areas, the threshold values are also exceeded at δ_x > +10 µm and < -20 µm (Fig. 5 a). A tangential misalignment of the forming rollers is also characterized by larger average channel heights of transversal channels (section D) when δ_x = ±10 µm is exceeded. Similar to the explanations for axial misalignment, the locally changed rolling gaps also lead to alternating larger and smaller thicknesses in the channel flanks (Fig. 5 c).

Angular misalignment.

The influence of an angular misalignment δ_α of the forming rollers was evaluated analogously by several simulations with different angular positions of the upper roller. To ensure comparability with the misalignment types, δ_x was changed in radian increments of 10 µm for the roller diameter of 105 mm, which corresponds to an angular value of 0.011°. As expected, the resulting sensitivities are comparable to those of tangential misalignment (Fig. 6 a).

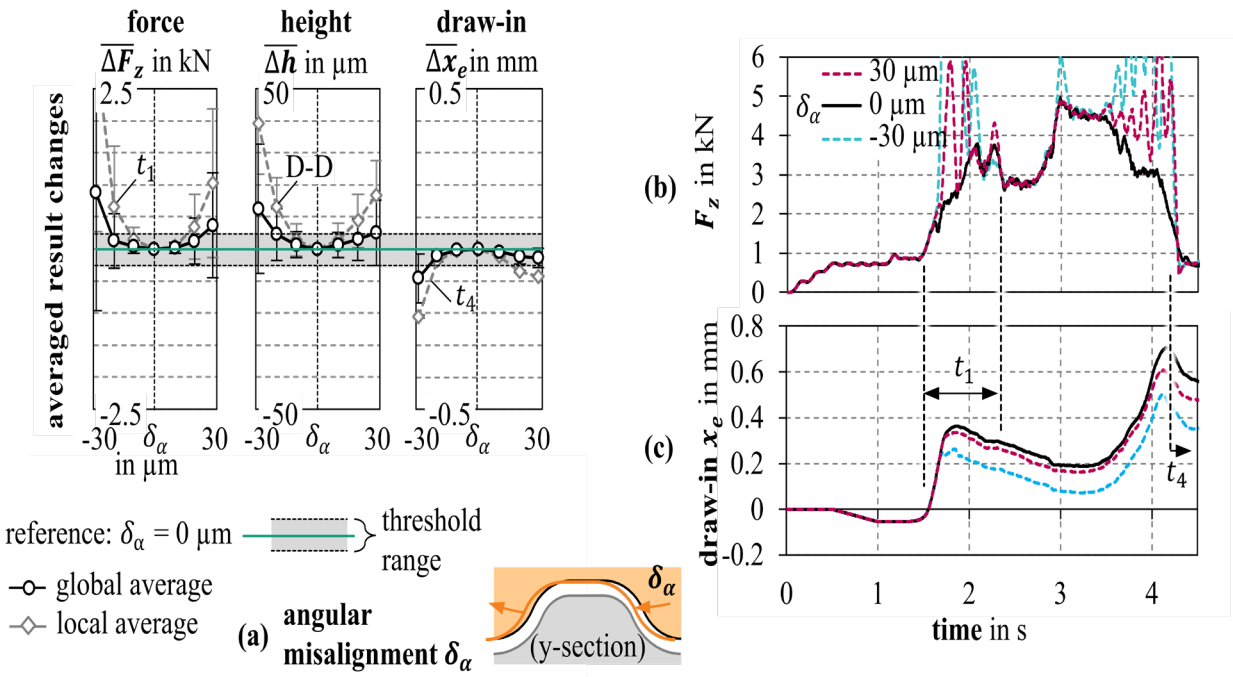

Fig. 6. Effects of angular misalignment: (a) significant changes of evaluation criteria, (b) exemplary change of rolling force, (c) exemplary change of longitudinal draw-in.

Again, significantly higher rolling forces (Fig. 6 b) and channel heights in transverse channel areas for δ_α < -10 µm and > +20 µm can be observed. The difference between positive and negative angular misalignment also arises here due to the different situation in the rolling gap. With a negative angular misalignment δ_α and a positive tangential misalignment δ_x, the rolling gap of the firstly formed transversal channel flank is reduced, resulting in a higher increase in rolling force than an equivalent rolling gap reduction of the subsequent transversal channel flank. A tangential misalignment of δ_α < -10 µm and > +20 µm is also associated with significant changes in longitudinal draw-in (Fig. 6 c). Due to the narrower rolling gap, a lower longitudinal draw-in is observed at the beginning of channel forming (t_1) with a negative angular misalignment.

Initial sheet thickness variation.

For a comprehensive evaluation of process robustness, the effect of an initial thickness change δt_0 in the range of ± 15 µm was also analyzed as a further possible process-specific disturbance variable. As expected, this results in significant rolling gap changes equivalent to the change in sheet thickness ($\Delta s_w \sim \delta t_0$). Even at only δt_0 = +5 µm, a significant increase in rolling forces can be observed (Fig. 7 a). On the one hand, the force required to form an identical channel geometry generally increases with higher initial sheet thickness; on the other hand, a clamping effect increasingly occurs in the flanks (Fig. 7 b). Since the meshes of the roller segments are identical, there are no changes in the predicted channel heights. Further significant changes in the results can already be observed for δt_0 < -10 µm and > +5 µm for the transversal edge draw-in y_e. This edge draw-in reduces with increasing initial sheet thickness, as more resistance is caused by the thicker strip drawing into the outer channel of the surrounding sealing bead. Significant changes in results due to a sheet thickness change of δt_0 > ±5 µm can also be observed for the longitudinal draw-in x_e. This is mainly caused by a generally reduced longitudinal draw-in of the strip when the first transversal channel is formed with a higher initial sheet thickness. Furthermore, higher plastic strains in longitudinal direction already occur in the middle plate area decreasing longitudinal draw-in as well. The significantly affected draw-in behavior in the transversal and longitudinal directions also correlates with the changed results of wrinkling criterion $\Delta\varepsilon_{WT}$ according to [6]. For δt_0 = +15 µm, wrinkling critical areas are much smaller than for δt_0 = -15 µm (Fig. 7 c).

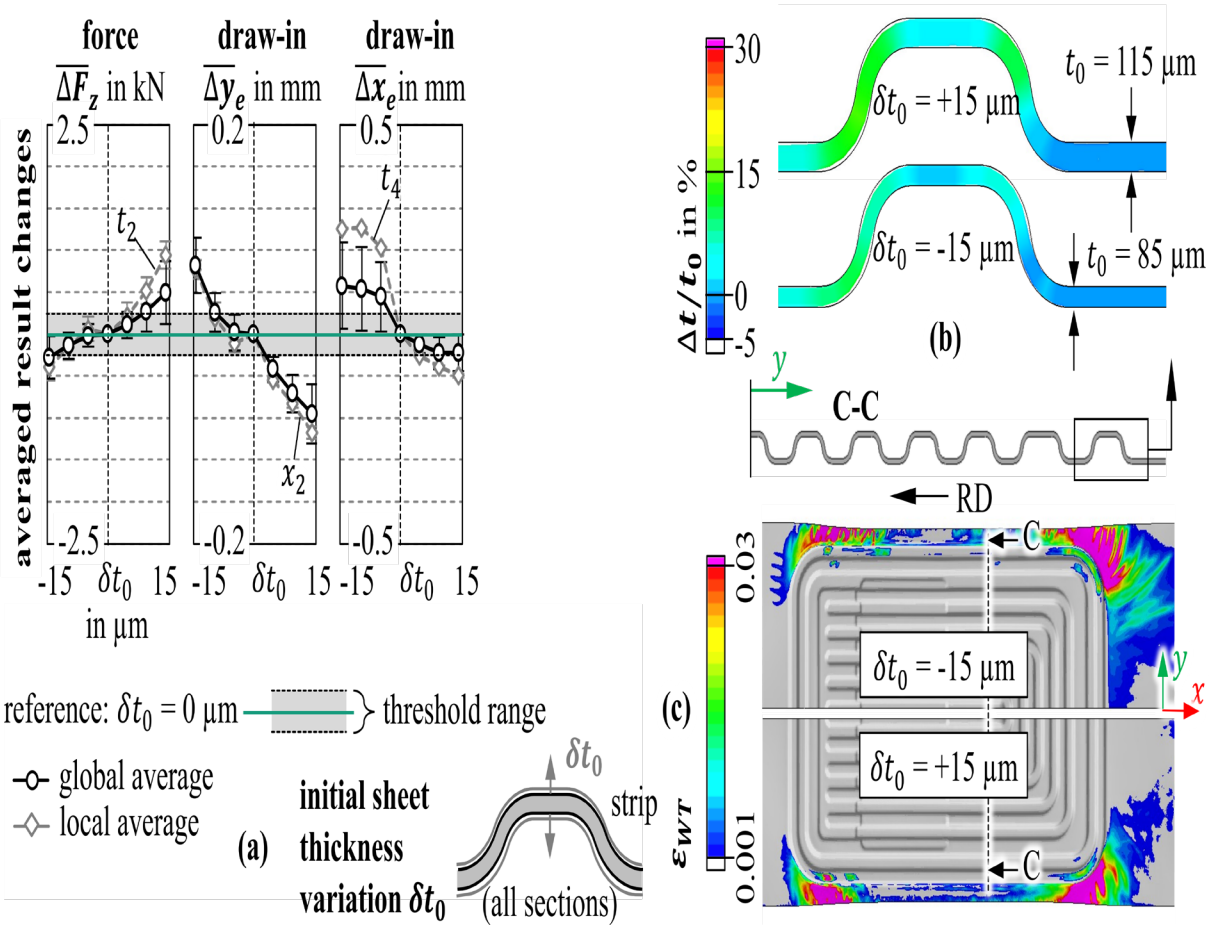

Fig. 7. Effects of initial thickness variation: (a) significant changes of evaluation criteria, (b) exemplary change of cross-sectional situation, (c) exemplary change of wrinkling tendency.

Roller gap variation due to manufacturing inaccuracies.

As the machining of such fine channel cross-sections is usually associated with tolerances in the range of ± 10 µm, the variation in the rolling gap due to manufacturing inaccuracies is another potential disturbance variable for HER. The changes in the results compared to the reference simulation are therefore analyzed when the upper die roller is provided with a uniform offset δs_w of ± 15 µm. The resulting rolling gap in the channel area with an identical lower punch roller is thus $s_w = t_0 - \delta s_w$ (Fig. 8 b). In general, similar result sensitivities can be observed as in the influence analysis of a sheet thickness change (Fig. 8 a). Firstly, the significant increase in rolling forces at $\delta s_w > 0$ resulting from the reduction in the effective rolling gap is remarkable. The corresponding threshold value (~5 % of the reference value) is already reached at δs_w = +5 µm, meaning that a manufacturing-related rolling gap decrease of 5 µm already results in significant rolling force increase. As expected, the load-dependent rolling gap change also increases with higher offset δs_w. The narrower rolling gap tends to result in lower sheet thicknesses in the channel flanks and head and foot areas. The threshold value for the change in results is reached here on average at δs_w = ± 15 µm, whereby standard deviations already indicate significant local changes in results at lower values of δs_w. Both the transversal edge draw-in and the longitudinal strip draw-in are also reduced as a result of a decreasing rolling gap and reach the corresponding threshold values at δs_w = +5 µm. While flatness deviation remains almost unchanged in the clamped state, there is also a significant increase in flatness deviation in the unclamped state for $\delta s_w > 5$ µm. Fig. 8 a also shows that negative values for δs_w, resulting in a larger rolling gap between the rollers due to manufacturing inaccuracies, generally do not lead to any significant changes in the simulation results.

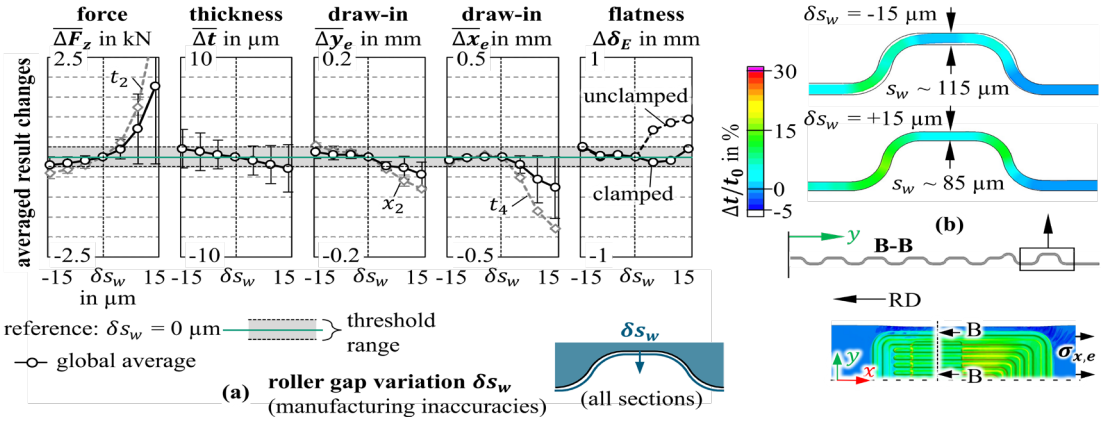

Fig. 8. Effects of roller gap variation: (a) significant changes of evaluation criteria, (b) exemplary change of cross-sectional situation.

Coefficient of friction variation.

Experimental studies on model validation have already shown that static friction coefficients of μ_s = 0.25 occur due to scaling effects of microforming in the HER of BPHP and have a major influence on the forming results [5]. For this reason, possible process-related variations in the static friction coefficient $\delta\mu_s = \pm 0.15$ are finally analyzed, which can arise, for example, due to varying surface roughness or inhomogeneous lubricant supply. The resulting friction coefficient is $\mu_s = 0.25 + \delta\mu_s$, covering a range from 0.1 to 0.4. Unlike previous results, such parameter variation causes only a slight change in the rolling forces below the threshold value. However, the influence on the thinning behavior of the strip in the channel cross-sections is much more significant. As expected, a higher coefficient of friction leads to more pronounced thinning in the channel flanks and less thinning in the channel head and foot areas, as the higher frictional forces inhibit flow from these flat areas (Fig. 9 a). The threshold value for the change in results is exceeded on average from $\delta\mu_s = \pm 0.1$, although standard deviations already indicate significant changes in the sheet thickness results even with minor changes in the friction coefficient. As a result of a changed coefficient of friction, significant changes in the results also occur with regard to transversal (Fig. 9 b) and longitudinal strip draw-in. Even at $\delta\mu_s = \pm 0.05$, the corresponding threshold value for the change in results is exceeded. Higher coefficients of friction and the associated higher frictional forces reduce the resulting transversal and longitudinal strip draw-in, which also reduce wrinkling-critical areas in the surrounding flange area (Fig. 9 c). Particularly at lower coefficients of friction ($\delta\mu_s < 0$), a clear increase in the predicted flatness deviation can also be observed, which can primarily be attributed to generally reduced stretching effects in the longitudinal and transverse directions of the strip. In contrast, no significant changes in flatness deviations occur at higher friction coefficients ($\delta\mu_s > 0$).

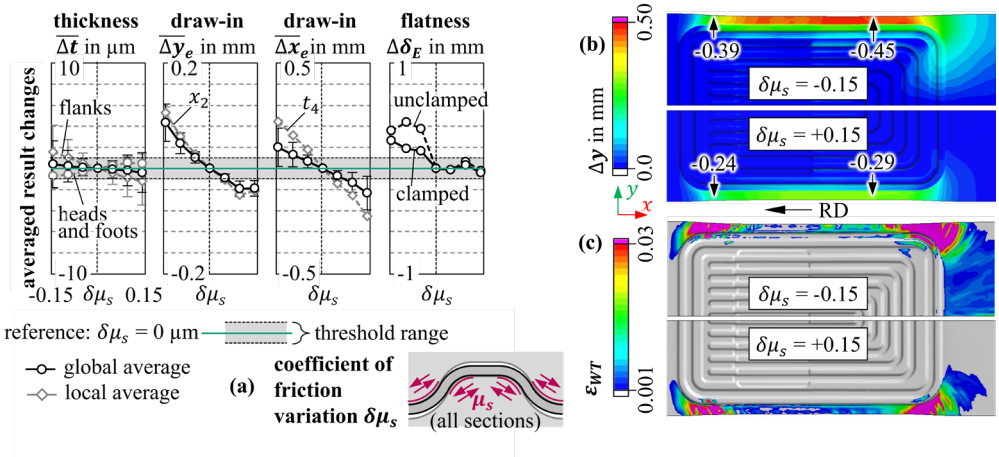

Fig. 9. Effects of coefficient of friction variation: (a) significant changes of evaluation criteria, (b) exemplary change transversal draw-in, (c) exemplary change of wrinkling tendency.

Limitations.

It is important to note that the idealized conditions of FE models, particularly in shell-based meshing and contact modeling, are typically associated with limitations and model errors. Although the qualitative correlations are entirely plausible, quantitative values should be further validated through extended experimental studies.

Summary

In this study, the effects of process-specific disturbances in hollow embossing rolling (HER) were investigated for continuous production of bipolar half plates (BPHP) with complex channel geometries. Using previously optimized and validated FE models, the effects of roller misalignments, roller gap and sheet thickness variations as well as changing friction coefficients were analyzed on process-relevant evaluation criteria of HER. In summary, it was demonstrated that a forming roller misalignment of ±10 µm leads to significant changes in results above the defined threshold values for the ideal reference state. This is mainly caused by increasing rolling forces as a result of locally narrower rolling gaps. Depending on the type of misalignment, channels oriented either longitudinally or transversely to the rolling direction will exhibit changes in the rolling gaps of the channel flanks. Significant changes in the results compared to the reference case can then be observed both in terms of thinning effects of the channel flanks and in terms of the transversal and longitudinal strip draw-in. The influence of roller misalignment should not only be evaluated as a possible quality-impairing disturbance variable in BPHP forming, but also in terms of minimizing tool load and wear effects. Similar effects were caused by changes in initial sheet thicknesses and reduced rolling gaps due to manufacturing inaccuracies, also leading to a change in rolling force due to the changed situation in the rolling gaps. From a technological point of view, reduced rolling gaps due to manufacturing inaccuracies are particularly critical. Even an oversize of only δs_w = +5 µm already affects the evaluation criteria significantly. In this case, the required rolling force increases by 5 % compared to the ideal reference simulation. Accordingly, very tight manufacturing tolerances of ± 5 µm are recommended for the forming rollers in order to provide ideal conditions for the HER process. Further investigations on the influence of the coefficient of friction also confirm significant effects on the evaluation criteria of thinning, strip draw-in, and the resulting flatness deviation. From a technological point of view, smaller coefficients of friction, for example caused via additional lubrication, are generally associated with negative effects, as the increased longitudinal and transverse draw-in results in a smaller locally strip stretching, which then becomes visible in the form of more pronounced wrinkling tendencies and flatness deviations.

References

[1] Porstmann, S., Wannemacher, T., Drossel, W.-G., 2020. A comprehensive comparison of state-of-the-art manufacturing methods for fuel cell bipolar plates including anticipated future industry trends. J. Manuf. Process. 60, 366–383.

[2] Reuther, F., Melzer, S., Geist, A., Polster, S., Psyk, V., 2024. Iterativer Designprozess für hohlprägegewalzte Elektrolyseurplatten am Beispiel von „HyVentus“. FC³ FUEL CELL CONFERENCE 2024, 12 November 2024, Chemnitz.

[3] Abeyrathna, B., Zhang, P., Pereira, M.P., Wilkosz, D., Weiss, M., 2019. Micro-roll forming of stainless steel bipolar plates for fuel cells. Int. J. Hydrogen Energy 44 (7), 3861–3875.

[4] Bauer, A., Härtel, S., Awiszus, B., 2019. Manufacturing of Metallic Bipolar Plate Channels by Rolling. JMMP 3 (2), 48.

[5] Reuther, F., Dix, M., Kräusel, V., Psyk, V., Porstmann, S., 2024. Model validation of hollow embossing rolling for bipolar plate forming. Int J Mater Form 17 (2).

[6] Reuther, F., 2025. Simulation of hollow embossing rolling for full-scale bipolar plates, in: Material Forming: ESAFORM 2025. Material Forming. 05/07/2025. Materials Research Forum LLC, pp. 1972–1981.

[7] Heidrich, S., Wagner, M., Kurth, R., Reuther, F., Ihlenfeldt, S., 2025. Key Parameters in Hollow Embossing Rolling of Metallic Bipolar Plates, in: International Rolling Conference (IRC 2025) Conference Proceedings. International Rolling Conference 2025. 2025. Association for Iron & Steel Technology.

[8] Wagner, M., Alaluss, M., Langheinrich, J., Reuther, F., Kurth, R., Ihlenfeldt, S., 2024. Prozessüberwachung mittels maschineninhärenter Sensoren/Transparency improvement in hollow embossing rolling of metallic bipolar plates – Process monitoring by using machine-inherent sensors. wt 114 (01-02), 15–20.

[9] Porstmann, S., Polster, S., Reuther, F., Melzer, S., Nagel, M., Psyk, V., Dix, M., 2021. Objectives and fields of tension in the comparison of manufacturing processes for metallic bipolar plates. Fuel Cell Conference FC³, 2021, Chemnitz.

[10] Reuther, F., Psyk, V., Kräusel, V., Dix, M., 2023. Simulation of Hollow Embossing Rolling for Bipolar Plate Forming using LS-DYNA©. 14th European LS-DYNA Conference, 2023, Baden-Baden.